The AAPS Journal (2021) 23:48
DOI: 10.1208/s12248-021-00569-x

Research Article

Can Pharmacokinetic Studies Assess the Pulmonary Fate of Dry Powder Inhaler Formulations of Fluticasone Propionate?

Günther Hochhaus,[1,14] Mong-Jen Chen,[1,2] Abhinav Kurumaddali,[1] Uta Schilling,[1] Yuanyuan Jiao,[3] Stefanie K. Drescher,[1] Elham Amini,[1] Bhargava Kandala,[1] Christine Tabulov,[1] Jie Shao,[1] Brandon Seay,[4] Mutasim N. Abu-Hasan,[4] Sandra M. Baumstein,[3] Lawrence Winner,[5] Jagdeep Shur,[6] Robert Price,[6] Michael Hindle,[7] Xiangyin Wei,[7] Cynthia Carrasco,[8] Dennis Sandell,[9] Oluwamurewa Oguntimein,[10] Minori Kinjo,[10] Renishkumar Delvadia,[10,11] Bhawana Saluja,[10,12] Sau L. Lee,[13] Denise S. Conti,[10] and Jürgen B. Bulitta[3,14]

Received 3 October 2020; accepted 6 February 2021

Abstract. In the context of streamlining generic approval, this study assessed whether pharmacokinetics (PK) could elucidate the pulmonary fate of orally inhaled drug products (OIDPs). Three fluticasone propionate (FP) dry powder inhaler (DPI) formulations (A-4.5, B-3.8, and C-3.7), differing only in type and composition of lactose fines, exhibited median mass aerodynamic diameter (MMAD) of 4.5 μm (A-4.5), 3.8 μm (B-3.8), and 3.7 μm (C-3.7) and varied in dissolution rates (A-4.5 slower than B-3.8 and C-3.7). *In vitro* total lung dose ($TLD_{in\ vitro}$) was determined as the average dose passing through three anatomical mouth-throat (MT) models and yielded dose normalization factors (DNF) for each DPI formulation X ($DNF_x = TLD_{in\ vitro,x}/TLD_{in\ vitro,A\text{-}4.5}$). The DNF was 1.00 for A-4.5, 1.32 for B-3.8, and 1.21 for C-3.7. Systemic PK after inhalation of 500 μg FP was assessed in a randomized, double-blind, four-way crossover study in 24 healthy volunteers. Peak concentrations (C_{max}) of A-4.5 relative to those of B-3.8 or C-3.7 lacked bioequivalence without or with dose

[1] Department of Pharmaceutics, College of Pharmacy, University of Florida, 1345 Center Drive, Gainesville, Florida, 32610, USA.
[2] *Present Address:* AbbVie Inc., North Chicago, Illinois, USA.
[3] Department of Pharmacotherapy and Translational Research, College of Pharmacy, University of Florida, 6550 Sanger Road, Gainesville, Florida 32827-7445, USA.
[4] Division of Pediatric Pulmonary and Sleep Medicine, Department of Pediatrics, College of Medicine, University of Florida, Gainesville, Florida, USA.
[5] Department of Statistics, College of Liberal Arts & Sciences, University of Florida, Gainesville, Florida, USA.
[6] Department of Pharmacy & Pharmacology, Centre for Therapeutic Innovation, University of Bath, Bath, UK.
[7] Department of Pharmaceutics, Virginia Commonwealth University, Richmond, Virginia, USA.
[8] Worldwide Clinical Trials, Austin, Texas, USA.
[9] S5 Consulting, Blentarp, Sweden.
[10] Office of Research and Standards, Office of Generic Drugs, Center for Drug Evaluation and Research, US Food and Drug Administration, Silver Spring, Maryland, USA.
[11] *Present Address:* Office of New Drug Products, Office of Pharmaceutical Quality, Center for Drug Evaluation and Research, US Food and Drug Administration, Silver Spring, Maryland, USA.
[12] *Present Address:* Office of Clinical Pharmacology, Office of Translational Sciences, Center for Drug Evaluation and Research, US Food and Drug Administration, Silver Spring, Maryland, USA.
[13] Office of Testing and Research, Office of Pharmaceutical Quality, Center for Drug Evaluation and Research, US Food and Drug Administration, Silver Spring, Maryland, USA.
[14] To whom correspondence should be addressed. (e–mail: hochhaus@ufl.edujbulitta@cop.ufl.edu)

Abbreviations: *API*, Active pharmaceutical ingredient; *APSD*, Aerodynamic particle size distribution; AUC_{0-Inf}, Area under the plasma concentration time curve from time zero until time infinity; AUC_{0-last}, Area under the plasma concentration time curve from time zero until the last observed plasma concentration; *AIT*, Alberta Idealized Throat; *BE*, Bioequivalence; *BSV*, Between subject variability; C_{max}, Observed peak concentration in plasma; *CV*, Coefficient of variation; *D50*, Median particle diameter; *DD*, Delivered dose; *DNF*, Dose normalization factor; *DPI*, Dry powder inhaler; *ECG*, Electrocardiogram; *EDTA*, Ethylene diamine tetra-acetic acid; *FEV1*, Forced expiratory volume in one second; *FP*, Fluticasone propionate; *FPD<3 μm*, Fine particle dose less than 3 μm; *FPD<5 μm*, Fine particle dose less than 5 μm; *GSD*, Geometric standard deviation; *HPLC/UV*, High performance liquid chromatography with ultraviolet detection; *IND*, Investigational new drug; *LC-MS/MS*, Liquid chromatography - tandem mass spectrometry; *MMAD*, Median mass aerodynamic diameter; *MAT*, Mean absorption time; *MDT*, Mean dissolution time; *MOC*, Micro-orifice collector; *MRT*, Mean body residence time; *MT*, Mouth-throat models; *NGI*, Next generation impactor; *PIFR*, Peak inspiratory flow rate; *PK*, Pharmacokinetics; *OPC*, Oropharyngeal consortium throat; *OIDPs*, Orally inhaled drug products; *RH*, Relative humidity; *SAP*, Statistical analysis plan; $TLD_{in\ vitro}$, *In vitro* total lung dose; T_{max}, Time to peak concentrations; *VCU*, Virginia Commonwealth University; *WSV*, Within subject variability.

Published online: 25 March 2021

normalization. The area under the curve (AUC_{0-Inf}) was bio-IN-equivalent before dose normalization and bioequivalent after dose normalization. Thus, PK could detect differences in pulmonary available dose (AUC_{0-Inf}) and residence time (dose-normalized C_{max}). The differences in dose-normalized C_{max} could not be explained by differences in *in vitro* dissolution. This might suggest that C_{max} differences may indicate differences in regional lung deposition. Overall this study supports the use of PK studies to provide relevant information on the pulmonary performance characteristics (i.e., available dose, residence time, and regional lung deposition).

KEY WORDS: bioequivalence of generic inhaled drugs; dry powder inhalers; fluticasone propionate; pharmacokinetics; regional lung deposition.

INTRODUCTION

To date, only one generic dry powder inhaler (DPI) product is available on the US market, in part due to challenges related to establishing equivalence for regulatory approval of complex, locally acting generic DPI products. For DPI products, *in vitro* studies (for equivalence in product performance) and *in vivo* studies (pharmacokinetic [PK] for equivalence in systemic exposure and comparative clinical pharmacodynamic [PD] or endpoint for equivalence in drug delivery at the sites of action) are recommended. This is in addition to formulation sameness (Q1 and Q2, i.e., the same inactive ingredients [Q1] and at the same concentration ± 5% as the reference product [Q2]) and device similarity, within the current weight-of-evidence approach (1–3). The main rationale for this rather complex approval pathway for DPI products is that plasma concentrations are downstream of the lung (i.e., the organ to which the drug is delivered to). Therefore, comparative clinical (PD or endpoint) studies are currently recommended by the US FDA to directly assess equivalence in local drug delivery for DPI products.

Comparative clinical (PD or endpoint) studies are generally less sensitive to product differences than PK studies, because of the flat dose-response relationships, especially for inhaled corticosteroids (4). Such comparative clinical (PD or endpoint) studies are further a challenge to pass because of the large inter- and intra-subject variabilities associated with these studies and the need to show equivalence of the effect (contrary to clinical studies of new drugs in which they "only" have to show efficacy against placebo) (5). The complexity, large sample size, long time required to perform these studies, the financial burden, as well as the associated risk of failing have been recognized by stakeholders. This has led FDA to perform research within the Critical Path Initiatives and the Generic Drug User Fee Amendments (GDUFA) Regulatory Science Program to evaluate alternative methodologies for establishing bioequivalence (BE) of OIDPs (6, 7).

An ideal alternative method to comparative clinical (PD or endpoint) studies needs to be able to evaluate three key *in vivo* performance measures of OIDPs—(i) the dose available to the lung, (ii) the time the drug stays in the lung (i.e., the pulmonary mean residence time), and (iii) the regional lung deposition (i.e., where the drug "lands" in the lung) (8). Prior PK simulations (9) suggest that PK studies should be able to detect differences in the pulmonary available dose (i.e., the amount of drug absorbed from the entire lung into the systemic circulation) by comparing the area under the plasma concentration time curves (AUC_{0-Inf}) and the peak plasma concentration (C_{max}) of test (T) and reference (R) products. Likewise, for typical drug-lactose inhalation powder dosage forms, differences in the pulmonary residence time should be detectable from plasma C_{max} and time to reach C_{max} (T_{max}). The pulmonary residence time is an important metric for the degree of pulmonary targeting (10), e.g., related to differences in dissolution rates of T and R products. Further, for slowly dissolving drugs, differences in dissolution rate might also result in differences in AUC, because more slowly dissolving drugs are expected to be more efficiently removed from the central lung through mucociliary clearance. As differences in dissolution rate affect AUC and C_{max}, the DPI formulation development in this study sought to ensure that dissolution properties were constant across the DPI formulations.

For slowly dissolving drugs, such as lipophilic corticosteroids (11), these PK simulations further supported the hypothesis that a formulation which deposits drug particles more centrally yields a smaller AUC_{0-Inf}, even though comparing two formulations that provide the same dose to the lung. This is caused by the central regions of the lung being protected by mucociliary clearance as an innate defense mechanism (9) for removal of solid particles. Thus, if slowly dissolving drug particles are deposited more centrally, they will be more efficiently removed by mucociliary clearance. This results in a more efficient removal of a fraction of the centrally deposited dose, a decreased extent of absorption, and a smaller AUC_{0-Inf} when compared to more peripherally depositing formulations. Moreover, differences in regional deposition may also affect C_{max}, as transcellular absorption of lipophilic drugs is assumed to be faster from the peripheral lung due to a larger surface area, more pronounced perfusion, and thinner epithelial membranes (12).

To test experimentally whether PK can detect differences in regional deposition, three carrier-based dry powder inhaler (DPI) formulations of fluticasone propionate (FP) were designed to achieve deposition in different regions of the lung (i.e., central *vs.* peripheral), but providing similar lung doses (i.e., similar amounts of drug depositing in the lung). All three DPI FP formulations were prepared using the same batch of API (FP) to achieve similar dissolution rates for all three formulations. These DPI FP formulations were cGMP manufactured and thoroughly characterized by multiple *in vitro* tests, followed by a randomized, double-blind, four-way crossover PK study in 24 healthy volunteers. For the lipophilic model drug FP, this study indicated that PK may be able to provide pertinent information related to the three key questions for assessing equivalence in drug delivery at the sites of action of OIDPs.

MATERIALS AND METHODS

Preparation of FP DPI Formulations

Four different inhalation grades of lactose were obtained from DFE Pharma (Goch, Germany). Respitose SV003 served as a coarse lactose carrier for all three DPI FP formulations (median particle diameter, D50: 63.6 μm), while micro-fine lactose LH300 (D50 < 5 μm) and two different grades of milled lactose fines (LH230 (D50 < 10 μm) and LH201 (D50: 20–25 μm)) were used to control the agglomeration behavior and thus the fine particle characteristics. A single batch of micronized FP (volume-weighted median diameter of 2.1 μm and 90% undersized particle size of 4.0 μm, obtained from Perrigo API Ltd, Bnei Brak, Israel) was used for all DPI formulations. All other chemical compounds were of analytical grade.

DPI formulation batches of 150 g were prepared by Catalent (Morrisville, NC, USA) under current Good Manufacturing Practice (cGMP) conditions. A series of lactose pre-blends were prepared and subsequently blended with FP (formulation A, LH201, SV003, and FP at concentrations of 19.8, 79.4, and 0.8 wt.%, respectively; formulation B, LH230, SV003, and FP at concentrations of 9.9, 89.3, and 0.8 wt.%; formulation C, LH300, SV003, and FP at concentrations of 2.5, 96.7, and 0.8 wt.%) with the drug content uniformity of the resulting FP-lactose blends, being measured according to USP<905> (13). These formulations were subsequently filled into size 3 hydroxypropyl methylcellulose (HPMC) capsules either through manual hand-filling or using a Quantos filling system to achieve a total capsule content of 100 μg FP in 12.4 mg of lactose carrier and subsequently stored at room temperature in a climatized environment. As the single dose for the PK study was five capsules (i.e., 5 x 100 μg FP), a total of five capsules were filled into high-density polyethylene (HDPE) bottles (Wheaton, Part No. 06-451-7) and individually foil-pouched (M-8407, 4 x 6", Pechiney Plastic Packaging).

In Vitro Characterization of FP DPI Formulations

Aerodynamic particle size distribution (APSD) of FP DPI formulations was characterized according to USP<601> (14). A next generation impactor (NGI), the compendial USP induction port, pre-separator, and impactor stages were coated with 1% glycerol in methanol. A flow rate of 60 L/min was used in all NGI tests. Tests were performed with five capsules containing FP formulations for a given NGI determination. After every NGI determination, the NGI was disassembled, and each impactor stage (including the capsule, device, USP induction port, and pre-separator) was washed with mobile phase (as described below) and dissolved in appropriately sized volumetric flasks for HPLC analysis. A validated reversed phase HPLC/UV method (5 μm; Hypersil C18 column, Thermo Scientific, acetonitrile:methanol:water at ratio of 50:5:45 %v/v as mobile phase) was used for quantification of FP with UV detection at 232 nm. The APSD parameters (i.e., average of 3 to 5 NGI determinations per FP DPI formulation) were determined after the release (5 months after manufacturing), after 1, 3, 9, 12, and 20 months of storage at room temperature (25°C, 60% RH) and after 1 and 3 months of storage under accelerated conditions (40°C, 75% RH). MMAD and geometric standard deviation (GSD) were calculated by using a web-based MMAD calculator (the website was available during data analysis, but was recently removed from the World Wide Web by the author). The delivered dose through the NGI (DD_{NGI}) was calculated as the sum of deposited drug mass in the induction port, pre-separator, and from stage 1 to micro-orifice collector (MOC). The FPD < 3 (fine particle dose smaller than 3 μm) and FPD < 5 (fine particle dose smaller than 5 μm) were obtained from the cumulative aerosol size distributions using a Weibull function for interpolation at 3 and 5 μm (15).

Realistic aerosol characterization made use of a combination of anatomical airway geometries of mouth-throat (MT) models and inhalation profiles. The goal of these tests was to determine the *in vitro* based total lung dose ($TLD_{in\ vitro}$) for each FP DPI formulation. The $TLD_{in\ vitro}$ was subsequently used for dose normalization during the PK data analysis to account for potential differences in the lung doses received by the healthy volunteers when inhaling the three FP DPI formulations. Therefore, dose normalization factor (DNF) was determined for each formulation X as $DNF_x = TLD_{in\ vitro,x}/TLD_{in\ vitro,A\text{-}4.5}$. The realistic *in vitro* aerosol characterization test (16, 17) was performed within 1 month after the completion of the PK study with three anatomical MT models that were coated with silicone spray to prevent powder re-entrainment. The three MT models (the Virginia Commonwealth University (VCU) medium size (18), the oropharyngeal consortium (OPC; Emmace Consulting AB, Lund, Sweden) medium size (19), and the Alberta Idealized Throat (AIT; Copley Scientific, Nottingham, United Kingdom)) (20) were used along with an inhalation profile that was representative of the average peak inspiratory flow rate (PIFR) observed in the PK study population (120 L/min). The inhalation flow profile was characterized by a peak inspiratory flow rate (PIFR) of 122.7 L/min, with a time to PIFR of 0.5 sec, an inhalation time of 2.1 sec, an inhalation volume of 2.7 L, and an average flow rate of 77 L/min (21). Inhalation procedures were repeated for a given capsule to mimic the PK study. While the AIT is only available in one size, medium size VCU and OPC MT models were preferred over the small or large sizes replica to allow more representative studies with "typical, average" MT geometries.

The $TLD_{in\ vitro}$ represented the amount of drug mass passing through the MT model which was subsequently collected on filter paper. FP was extracted from the filter paper as previously described (16, 17). The amount of FP collected on filter paper, deposited in the MT model (obtained by washing the model with ethanol), and left in the device (obtained by washing the device with ethanol) was determined using a validated reversed phase HPLC/UV method (Hypersil GOLD C18 column, 3 μm, 4.6x100 mm, Thermo Scientific, acetonitrile:deionized water at a ratio of 60:40 %v/v as mobile phase, flow rate of 1.3 mL/min, UV detection at 230 nm, and injection volume of 100 μL). Calibration curves were linear from 0.2 to 10.0 μg/mL (r^2 > 0.999). Experiments were performed for a given MT model and FP DPI formulation in 5 replicates. Based on the results generated with VCU, OPC, and AIT MT models, the average ex-throat dose was calculated for each formulation X ($TLD_{in\ vitro,x}$). These average $TLD_{in\ vitro,x}$ estimates obtained

for each formulation X were used to calculate the relative dose normalization factors ($TLD_{in\ vitro,x}/TLD_{in\ vitro,A\text{-}4.5}$) using the average $TLD_{in\ vitro,x}$ of formulation A-4.5 ($TLD_{in\ vitro,A\text{-}4.5}$) as comparator.

Dissolution profiles for the collected respirable fraction (equivalent to $TLD_{in\ vitro}$ determined as the total drug mass passing through the MT model) of FP DPI formulations were assessed with a recently described dissolution method (22). An experimental set-up similar to that employed for estimating the $TLD_{in\ vitro}$ (described above) was used, with the exception of utilizing a constant air flow rate of 60 L/min rather than an inhalation profile and a filter holder that accepted a 24-mm glass microfiber filter paper (pore size of 1.2 μm, Whatman GF/C™). The dry filter paper, containing the deposited respirable fraction, was immediately transferred face up to the donor compartment of a Transwell® system (a six-well 24-mm Transwell® plate with 8 μm pore polycarbonate membrane inserts). The transferred samples were processed as described previously (23) using 0.5% Tween 80 in water (pH 7.4) as dissolution medium (with 1.4 mL in the receptor and 0.5 mL in the donor compartment) and frequent serial sampling/replenishment of 0.5 mL over 24 h. Drug content was assayed by reversed phase HPLC, as described previously (23).

In addition, dissolution tests were performed with the USP paddle apparatus. Drug particles collected in the same way as described above were attached face up to a glass disk and placed in the USP paddle apparatus (600 mL, 0.5% Tween 80 [filtered through a Whatman GF/C filter], 80 RPM, 37°C, 2.5 cm distance between glass disk and paddle). Samples (4 mL obtained after filtration through a poroplast cannula filter FIL001-HR) were taken through serial sampling/replenishment over 2 h and analyzed as described above. Results were expressed as fraction of dissolved drug over time. The mean dissolution time (MDT) was derived from the fraction of undissolved drug *vs.* time profiles as the ratio between area under the first momentum curve and the area under the undissolved drug time curve (22, 24). In addition to the MDT, the dissolution rate constant kd was calculated for the USP experiments from the fraction of undissolved drug *vs.* time profiles for the 3 to 30 min time window. This assumed a linear relationship between the logarithm of undissolved drug and dissolution time. The results obtained from the USP experiments were further used in the PK simulations described below.

Pharmacokinetic Study

Study Ethics. The PK study (ClinicalTrials.gov identifier number NCT #01966692) was conducted in compliance with Good Clinical Practice and the revised version of the Declaration of Helsinki. An investigational new drug (IND) application was approved by FDA (IND #123113). The study was approved by both the University of Florida and FDA Institutional Review Boards (UF-IRB and FDA-IRB, respectively) and was performed at the University of Florida Clinical and Translational Science Institute (UF-CTSI) clinical research center.

Study Design. A single-center, double-blind, randomized, four-way crossover PK study in adult, healthy volunteers with a washout period of at least 5 days. Each subject received the FP DPI formulations (A, B, C, and CR which was the replicate of C to assess intra-subject variability) in separate study periods. As described in more detail below, on a given study day, a total dose of 500 μg of FP, equivalent to 5 capsules each containing 100 μg FP, was administered.

Healthy male and female volunteers (18 to 50 years) with a body mass index (BMI) of 18 to 29 kg/m^2 were included. Subjects were required to be non-smokers since at least 12 months with no history of respiratory disease or other relevant conditions potentially affecting the study or PK results. These conditions were identified from the medical history, blood testing, physical examination, and electrocardiography. Subjects were required to have normal baseline spirometry (FEV1 and FVC, both at least 90% of predicted) as predicted by their age, sex, and height. Additionally, the ratio of forced expiratory volume in 1 second and forced vital capacity (FEV1/FVC), a ratio used in the diagnosis of obstructive and restrictive lung disease, had to show a value of at least 80% during the screening visit.

The main exclusion criteria were (i) intake of any medication that had the potential to alter drug metabolism via CYP3A4 within 2 weeks of dosing (e.g., azole antifungals or rifampin), (ii) donation of 450 mL blood or more within 8 weeks before period 1, or (iii) any known sensitivity (including allergies) to corticosteroids or the components of the FP DPI formulations. In order to minimize variability, subjects were trained by experienced clinical staff team members during screening and at the beginning of each study period using the Vitalograph Aerosol Inhalation Monitor (AIM)™. Subjects were required to demonstrate their ability to properly use the DPI device at the screening visit and each study visit.

Inhalation Profile Measurements. To enable recording the inhalation profiles of all subjects during the PK study, the capsule-based DPI device was modified by tightly attaching a specially designed ring adaptor to the mouthpiece. This adapter had an opening that was connected via silicone tubing to a calibrated pressure transducer (Phidgets, Calgary, Canada). The latter allowed digital recording of the pressure drop profile over time (in millisecond resolution) which was translated into inhalation flow rate profiles that were used to calculate PIFR, time to PIFR, and inhalation volume. Inhalation profiles were recorded for all subjects and all inhalation steps (i.e., two inhalations per each capsule, five capsules per study period, and four study periods).

Dosing. In addition to the inhalation training performed at the screening visit, subjects were re-trained at each study visit directly before dosing. Subjects inhaled subsequently the powder content from five capsules, each capsule containing 100 μg FP, via the modified DPI Monohaler 8® (Plastiape, Milan, Italy; for modifications, refer to the section "Inhalation Profile Measurement"). After each inhalation, subjects held their breath for 10 s (as per labeling of commercial fluticasone propionate and salmeterol xinafoate inhalation powder). To ensure complete dose delivery, each subject inhaled at least twice from each capsule, and the complete emptying of the capsule was assessed visually. In a few rare cases of visually incomplete capsule emptying, subjects were asked to inhale

from the unemptied capsule again. This inhalation steps required at least 10 inhalations from each subject, which typically took approximately 5 to 8 min.

Blood Sampling. Blood samples were taken using ethylene diamine tetra-acetic acid (EDTA) vacutainers within 30 min prior to the dosing and at 5, 10, 15, 20, 30, 45, 60 min, 1.5, 2, 3, 4, 6, 8, 10, 12, 14, and 24 h after the last inhalation of the fifth capsule. All actual inhalation and blood sampling times were recorded and used for PK data analysis. After centrifugation, plasma samples were immediately frozen and stored at −70°C until bioanalysis which happened after 2 months or sooner. Fluticasone propionate has been shown to be stable under these conditions (25).

Bioanalysis. Fluticasone propionate concentrations in plasma were quantified via a validated Liquid Chromatography - tandem Mass Spectrometry (LC-MS/MS) assay at Worldwide Clinical Trials (Austin, TX). The PK samples containing fluticasone propionate and the internal standard (i.e., deuterated FP, FP-D5) were extracted by liquid-liquid extraction and analyzed by a Sciex API 6500 (MS/MS transition: m/z 501.2 → 313.2). The inter- and intra-batch precision and accuracy for the quality control samples (1.5 pg/mL, 15 pg/mL, and 160 pg/mL) were both less than 15%. The lower limit of quantification was 0.5 pg/mL.

Data Analysis. A non-compartmental PK data analysis was performed using the Phoenix WinNonlin Professional software (Certara, Princeton, NJ, USA) (24). The area under the curve (AUC_{0-last}) was calculated by the linear-up/log-down rule, and the predicted plasma concentration at the last time point was used to extrapolate the area from this time point to infinity to calculate AUC_{0-Inf}. The C_{max}, AUC_{0-last}, and AUC_{0-Inf} were reported with and without dose normalization. Dividing C_{max}, AUC_{0-last}, and AUC_{0-Inf} estimates of a given FP DPI formulation X by the dose normalization factor DNF ($DNF_x = TLD_{in\ vitro,x}/TLD_{in\ vitro,A\text{-}4.5}$) allowed us to calculate dose-normalized PK parameter estimates. Statistical comparisons were performed using analysis of variance on log scale with treatment, period, sequence, and subject within sequence as factors in the SAS software (version 9.4, SAS Institute Inc., Cary, NC). Pair-wise treatment comparisons were performed using Bonferroni-adjusted p values at the 5% significance level. Bioequivalence demonstration was performed for log-transformed C_{max} and AUC_{0-Inf} using the established confidence interval limits of 80.00 to 125.00%.

PK Simulations. Assuming that dissolution is the rate-limiting step for absorption (23), the potential effects of differences in the dissolution rates of FP DPI formulations on C_{max} were assessed using an *in silico* PK simulation tool (26). A two-compartment body model with first-order absorption incorporated the PK parameters from this publication for FP (V_c, 31 L; Vd_{ss}. 646 L; Vd_{area}, 1440 L; and a clearance (CL) of 73 L/h) and absorption rate constants (k_a) of 1.0 through 1.55 h^{-1} (to mirror differences in MDT and kd, see also **Table I**). This PK model and parameter estimates were employed to predict the differences in C_{max} when absorption rate differences were caused by differences in the dissolution rates. We then systematically varied the absorption rate constants and predicted the C_{max} and the AUC_{0-Inf} while keeping all other model parameters constant. The model-predicted C_{max}/AUC_{0-Inf} ratios were then compared to the observed C_{max}/AUC_{0-Inf} ratios observed in the PK study. This ratio (i.e., C_{max} normalized by AUC_{0-Inf}) accounts for differences in the absorbed dose and therefore allowed us to study the impact of the absorption rate.

Table I. APSD Properties (Average of Samples Stored from 12 to 20 Months at Ambient Conditions (25°C, 60%) Within the Stability Program) and Mean Dissolution Time of FP DPI Formulations Obtained from *In Vitro* Compendial NGI and Dissolution Testing, Respectively

Parameters	FP DPI formulations		
	A-4.5	B-3.8	C-3.7
MMAD (μm)	4.50 (0.12)	3.78 (0.15)	3.72 (0.04)
GSD (μm)	1.89 (0.04)	2.01 (0.08)	2.05 (0.04)
FPD < 5μm (μg)	12.2 (1.0)	18.7 (0.9)	15.9 (0.9)
FPD < 3μm (μg)	5.28 (0.69)	9.98 (0.50)	8.60 (0.57)
NGI stages 2 to 3 (μg)	12.5 (0.7)	14.4 (1.3)	11.6 (0.6)
NGI stages 4 to 7 (μg)	4.83 (0.63)	9.37 (0.44)	8.17 (0.46)
FP left in capsule (μg)	15.3 (0.7)	6.87 (1.00)	5.08 (0.63)
FP left in device (μg)	12.0 (0.8)	7.52 (1.33)	6.79 (1.08)
DD_{NGI} (μg)	67.8 (5.4)	81.2 (2.2)	82.2 (1.4)
Mean dissolution time, MDT Transwell (h)	12.2 (2.8)	10.4 (2.5)	8.5 (2.3)
MDT USP (min)	23.4 (0.4)	20.5 (0.3)	17.8 (0.3)
Dissolution rate (kd) USP (min^{-1})	0.049 (0.010)	0.055 (0.016)	0.076 (0.021)

MMAD mass median aerodynamic diameter, *GSD* geometric standard deviation, *FPD* fine particle dose, *NGI* next generation impactor, *FP* fluticasone propionate, *DD* delivered dose. Values shown as mean (standard deviation) of n = 6 for A-4.5 and B-3.8 and n=5 for C-3.7 of samples of FP DPI formulations stored at room temperature for 12 and 20 months, which covers the duration of the PK study. n = 6 for dissolution experiments

RESULTS

Formulation and *In Vitro* Assessment

Using the same batch of FP, but differing amounts and particle size distributions of lactose fines, resulted in FP DPI formulations differing in *in vitro* behavior. Drug content uniformity of the resulting FP-lactose blends was 98.3 ± 1.7, 98.6 ± 2.1, and 95.9 ± 1.7% of label claim for formulations A, B, and C, respectively. Compendial NGI assessments obtained from 12 to 20 months after storage at room temperature (25°C, 60% RH) (the PK study was performed between these months) indicated that the MMAD of FP DPI formulation A was 4.5 μm, larger than that of formulations B (3.8 μm) and C (3.7 μm) (**Fig. 1, Tables I and II**). Therefore, from now on, the FP DPI formulations are reported by their MMAD values as A-4.5, B-3.8, and C-3.7. In agreement with this finding, other fine particle–related parameters (FPD < 5 μm, FPD < 3 μm) were smaller for formulation A-4.5 than those for formulations B-3.8 and C-3.7 (**Table II**) with stability of FPD<3 μm being similar to the stability of the FPD<5 μm over the investigated 20 months stability program (**Table II**). The latter two formulations showed similar APSD parameters (**Table I**). The amount of drug deposited on NGI stages 2 and 3 was relatively similar across the three formulations. However, the much smaller amount of drug deposited on stages 4–7 and MOC led to a larger MMAD for formulation A-4.5.

Stability tests over the 20-month period (**Table II**) indicated that MMAD and DD_{NGI} were comparatively stable over time for all three formulations. A decrease by approximately 20% (or less) was observed for the FPD < 5 μm and mainly occurred during the early storage. Subsequently, formulations remained relatively stable during the conduct of the PK study period (i.e., between 12 and 20 months of the stability program).

Experiments with Realistic, Anatomical MT Models and Inhalation Profile

The $TLD_{in\ vitro}$ shown in **Table III** generated with three realistic, anatomical MT models and one inhalation profile differed between the FP DPI formulations, mirroring the compendial results (e.g., FPD < 3 μm in **Table I**). However, when results obtained with the three MT models were compared directly, differences between the MT models were observed. The $TLD_{in\ vitro}$ for formulation A-4.5 ranged from 9.24 (VCU) to 17.7 μg (OPC). Estimates ranged from 13.2 (AIT) to 20.2 μg (OPC) for formulation B-3.8 and from 13.0 (VCU) to 17.9 μg (OPC) for formulation C-3.7. Not only the absolute amounts but also the ratios between the FP DPI formulations differed between MT models. As an example, the ratio of $TLD_{in\ vitro}$ between formulations A-4.5 and B-3.8 was 1.14 with the OPC MT model, whereas the VCU MT model suggested a $TLD_{in\ vitro}$ ratio of 1.8. Therefore, in the statistical analysis plan (SAP) of the PK study, it was pre-

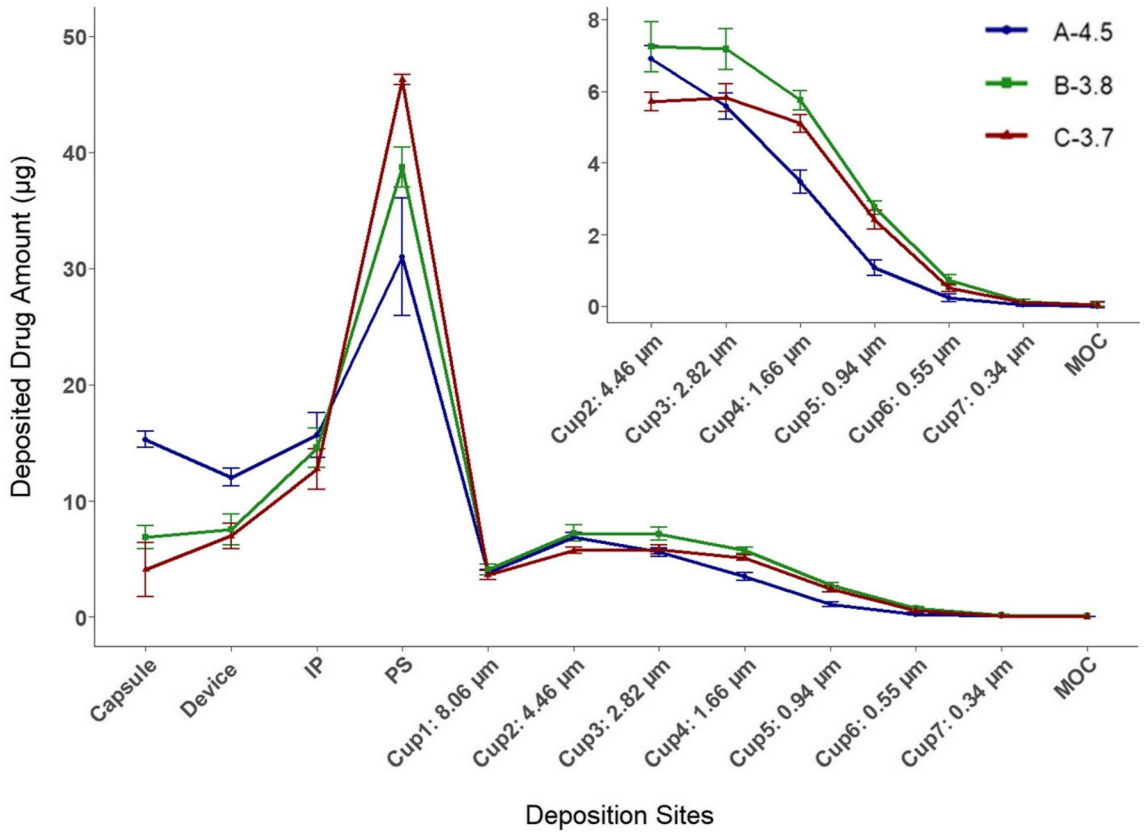

Figure 1. APSD deposition profiles from compendial NGI *in vitro* testing (mean ± standard deviation of at least 5 replicates; data combined from samples stored from 12 to 20 months at ambient conditions (25°C; 60% RH) which is a good representation of the FP DPI formulations administered in the PK study). IP, induction port; PS, pre-separator; MOC, micro-orifice collector

Table II. APSD Parameters from Compendial NGI Testing of FP DPI Formulations Assessed During the Conduct of Stability Program

Parameter	Formulation	Storage condition	Months after release of formulations					
			0	1	3	9	12*	20*
			Mean (SD)					
DD_{NGI} (μg)	A-4.5	25°C/60%	67.2 (1.8)	66.9 (2.2)	65.0 (1.6)	63.7 (2.5)	63.5 (1.9)	72.1 (3.6)
	B-3.8	25°C/60%	83.6 (0.8)	77.6 (2.3)	80.9 (2.8)	78.3 (2.9)	81.0 (0.7)	81.4 (3.4)
	C-3.7	25°C/60%	82.9 (1.4)	82.7 (0.6)	83.9 (2.2)	80.8 (3.2)	81.2 (0.3)	83.1 (1.3)
	A-4.5	40°C/75%		68.2 (0.6)	67.0 (0.9)			
	B-3.8	40°C/75%		83.7 (0.9)	83.1 (2.9)			
	C-3.7	40°C/75%		83.1 (0.5)	82.9 (1.1)			
FPD < 5 μm (μg)	A-4.5	25°C/60%	14.7 (0.8)	15.1 (0.6)	13.4 (0.7)	12.5 (0.5)	12.0 (0.3)	12.4 (1.6)
	B-3.8	25°C/60%	23.2 (0.5)	20.2 (0.9)	20.5 (1.6)	18.5 (0.8)	19.1 (1.1)	18.3 (0.7)
	C-3.7	25°C/60%	18.7 (0.7)	18.7 (0.7)	18.6 (1.2)	15.8 (0.9)	16.1 (0.7)	15.6 (1.1)
	A-4.5	40°C/75%		13.2 (0.2)	11.4 (0.5)			
	B-3.8	40°C/75%		21.4 (1.1)	19.4 (1.4)			
	C-3.7	40°C/75%		17.1 (0.6)	15.7 (1.0)			
FPD < 3 μm (μg)	A-4.5	25°C/60%	6.23 (0.40)	6.47 (0.17)	5.76 (0.26)	5.33 (0.26)	4.99 (0.12)	5.56 (0.96)
	B-3.8	25°C/60%	12.8 (0.4)	10.7 (0.6)	10.7 (1.3)	9.63 (0.66)	9.83 (0.49)	10.1 (0.6)
	C-3.7	25°C/60%	10.8 (0.3)	10.6 (0.4)	10.4 (0.5)	8.64 (0.52)	8.70 (0.23)	8.50 (0.78)
	A-4.5	40°C/75%		5.26 (0.10)	4.53 (0.21)			
	B-3.8	40°C/75%		10.6 (0.9)	9.60 (0.91)			
	C-3.7	40°C/75%		9.19 (0.29)	7.79 (0.58)			
MMAD (μm)	A-4.5	25°C/60%	4.30 (0.12)	4.22 (0.04)	4.40 (0.07)	4.46 (0.27)	4.60 (0.00)	4.47 (0.15)
	B-3.8	25°C/60%	3.54 (0.05)	3.60 (0.07)	3.78 (0.22)	3.60 (0.32)	3.90 (0.00)	3.63 (0.06)
	C-3.7	25°C/60%	3.40 (0.07)	3.40 (0.07)	3.52 (0.04)	3.62 (0.22)	3.75 (0.07)	3.70 (0.00)
	A-4.5	40°C/75%		4.64 (0.09)	4.86 (0.15)			
	B-3.8	40°C/75%		3.86 (0.09)	3.94 (0.05)			
	C-3.7	40°C/75%		3.60 (0.07)	3.90 (0.07)			

Five capsules of each FP DPI formulation were assayed for the 0th, 1st, 3rd, and 9th month. Three capsules of FP DPI formulations A-4.5 μm and B-3.8 μm and two capsules of C-3.7 μm were assayed for the 12th month. Three capsules of each FP DPI formulation were assayed for the 20th month. *Averages of the 12th and 20th month results (n=5) were used to describe the FP DPI formulations during the PK study period
Samples stored under ambient (25°C, 60% RH) and accelerated conditions (40°C, 75% RH)

specified that the final dose to be used in the PK data analysis should be normalized based on the $TLD_{in\ vitro}$ average of the three MT models for a given formulation. The observed ratios were subsequently converted into dose normalization factors (DNF); these factors were 1.00 for formulation A-4.5, 1.32 for B-3.8, and 1.21 for C-3.7 (**Table III**).

Dissolution Tests

Transwell®-based dissolution characterization showed the slowest dissolution rate for FP DPI formulation A-4.5 (**Fig. 2**). The latter had, on average, an MDT of 12.2 h, followed by formulations B-3.8 with an MDT of 10.4 h and C-3.7 with 8.5 h (**Table I**). The MDT estimates and dissolution rate constants obtained with the USP paddle apparatus (**Table I and Fig. 2**) showed similar differences between the FP DPI formulations with C-3.7 dissolving about 1.3–1.55 fold faster than formulation C-3.7 (**Table I**).

Pharmacokinetic Study

Adult healthy volunteers (n=24) were dosed in the PK study (see **Table IV** for demographics) and were trained on the proper inhalation technique using the DPI device. There were no drop-outs, and the FP DPI formulations were generally well tolerated with no serious adverse event. Subject inhalation profiles recorded during study visits showed a mean peak inspiratory flow rate (PIFR) of 120 L/min (range: 65.2 to 167 L/min), mean time to PIFR of 0.33 s (range: 0.05 to 0.97 s), mean inhalation time of 1.07 s (range: 0.39 to 2.11 s), and mean inhalation volume of 1.46 L (range: 0.26 to 3.27 L).

The mean plasma concentrations (**Fig. 3**) were near-identical for the FP DPI formulations B-3.8, C-3.7, and CR-3.7 which led to closely comparable PK parameters for these treatments (**Table V**). While terminal half-life was comparable between all three formulations, the mean residence time was slightly longer for formulation A-4.5. Formulation A-4.5 achieved considerably lower concentrations during the first 3 h and had smaller C_{max}, AUC_{0-last}, and AUC_{0-Inf} before dose normalization (**Table V**). Consequently, formulation A-4.5 was determined to be bio-IN-equivalent for all three PK parameters when data were not dose-normalized.

After dose normalization based on the DNF values, the C_{max}, AUC_{0-last}, and AUC_{0-Inf} of A-4.5 became more similar to the other two FP DPI formulations (**Table V**). Dose-normalized AUC_{0-last} and AUC_{0-Inf} passed bioequivalence criteria, whereas dose-normalized C_{max} continued to fail bioequivalence (**Table VI**). We further calculated the C_{max}/AUC_{0-Inf} ratios as an alternative approach to obtain dose-normalized peak concentrations (exploratory, since it was not

Table III. *In Vitro* Performance of FP DPI Formulations from Total Lung Dose ($TLD_{in\ vitro}$) Collected Using Three Different Mouth-Throat (MT) Models and One Inhalation Profile (IP)

Mouth-throat model	Formulations	FP retained in device (μg)	FP deposited in MT (μg)	$TLD_{in\ vitro}$ (μg)	$TLD_{in\ vitro}$ ratio[a]
VCU medium (*n*=10)	A-4.5	28.2 (3.5)	48.8 (5.1)	9.24 (1.34)	1.00
	B-3.8	15.4 (2.3)	62.0 (1.5)	16.7 (1.9)	1.81
	C-3.7	14.9 (2.1)	66.2 (2.6)	13.0 (1.6)	1.41
AIT (*n*=5)	A-4.5	32.6 (1.9)	44.9 (2.4)	11.4 (1.0)	1.00
	B-3.8	14.4 (1.3)	51.4 (6.5)	13.2 (2.0)	1.16
	C-3.7	15.9 (5.8)	64.3 (6.6)	14.8 (2.4)	1.30
OPC medium (n=5)	A-4.5	26.5 (4.2)	36.1 (2.4)	17.7 (1.0)	1.00
	B-3.8	14.3 (2.7)	54.3 (0.2)	20.2 (1.7)	1.14
	C-3.7	16.4 (6.9)	56.2 (7.7)	17.9 (1.7)	1.01
Average of three MT models[b]	A-4.5			12.8	1.00
	B-3.8			16.7	1.32
	C-3.7			15.2	1.21

VCU medium, Virginia Commonwealth University medium MT model; AIT, Alberta Idealized MT model; OPC medium, oropharyngeal consortium medium MT model. [a] Referred to as "dose normalization factor (DNF)" in the text. [b] *Calculated as the ratio of the average of the $TLD_{in\ vitro}$ from VCU, AIT, and OPC with FP DPI formulation A-4.5um being the reference*
Values shown as mean (standard deviation) of *n* samples indicated below

described in the SAP). The C_{max}/AUC_{0-Inf} ratio of formulation A-4.5 (derived from C_{max} and AUC_{0-Inf} estimates of **Table V** before dose normalization) was approximately half compared to the ratios of the other formulations. When we employed a two-compartment body model for PK simulations, the model predicted that a 1.3- to 1.55-fold increase in the absorption rate constant (in accordance with the observed differences in MDT or kd of **Table I**) would only result in a 19 to 34% increase in the C_{max}/AUC_{0-Inf} ratio.

DISCUSSION

This study was originally attempting to prepare FP DPI formulations that were similar in delivered dose (DD), dissolution kinetics, and pulmonary deposited dose, but would differ in MMAD and, consequently, in regional lung deposition. Our ultimate goal was to investigate whether PK is able to distinguish between FP DPI formulations that differ in regional deposition. We used DPI formulations instead of nebulized formulations because of their relevance for bioequivalence assessments of oral inhalation products currently of interest for the generic industry.

By using the same batch of FP (API) for all three formulations, we further intended to ensure similar dissolution characteristics. This formulation strategy was intended to facilitate testing of our hypothesis that DPI formulations of slowly dissolving drugs that are deposited more centrally in the lung achieve smaller C_{max} and AUC_{0-Inf} in plasma due to a more extensive impact of mucociliary clearance. Thus, AUC differences were hypothesized, even if these FP DPI formulations would provide the same total lung doses.

Previous work (27–29) suggested that fine particle dose (or fraction) and MMAD of DPI formulations may be controlled by blending the API with different grades and amounts of lactose fines. This affects the performance of carrier-based DPI formulations by modulating the fluidization and drug-lactose fine agglomerate formation (29–31). More lactose fines increased the MMAD and FPD of budesonide DPI formulations (27), while other studies suggested a decrease in FPD and increase in MMAD when both the amount of lactose fines and their particle size distribution were increased, as reviewed by Peng and colleagues (32).

For the FP DPI formulations in the present study, although challenging, we simultaneously modulated the lactose fine content and their particle size to achieve, if

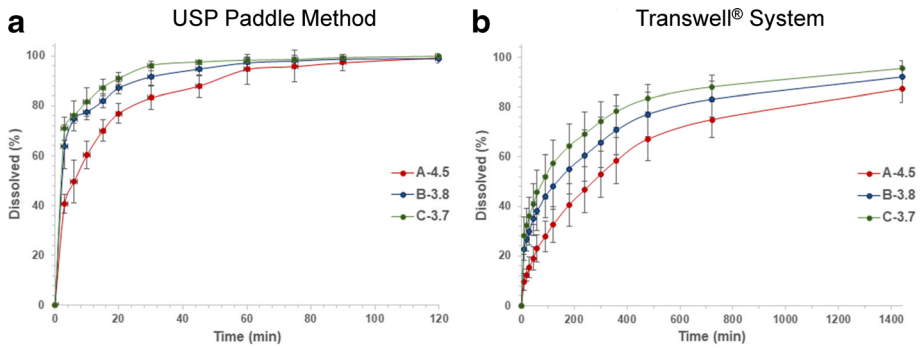

Figure 2. Dissolution of FP DPI formulations. Percent dissolved (mean ± standard deviation) of FP DPI formulations A-4.5, B-3.8, and C-3.7 using either the USP paddle apparatus (**a**) or the Transwell® system (**b**)

Table IV. Subject Demographics of the PK Study

Characteristic	Results
Age, years	23 (18–48)
Sex	
Female (*N*)	13
Male (*N*)	11
Weight, kg	64.6 (50.2–75.1)
Height, cm	167 (155–180)
BMI, kg/m^2	23.2 (18.6–28.8)
Study population (%)	
Asian	33.3
African American	45.8
Caucasian	20.8
FEV1, L	3.46 (2.45–4.36)
FVC, L	3.98 (2.75–5.17)
FEV1/FVC	0.86 (0.81–0.93)

BMI body mass index, *FEV1* forced expiratory volume in 1 second, *FVC* forced vital capacity. Data in parenthesis represent range (min–max). *N* stands for number of subjects that completed the PK study

possible, a similar *in vivo* lung dose while at the same time achieving differences in MMAD. We were only partially successful as two of our three FP DPI formulations (B-3.8 and C-3.7) had comparable MMADs (3.8 and 3.7 μm, respectively), whereas the FP DPI formulation A-4.5 showed larger MMAD (4.5 μm). However, based on *in vitro* surrogates of lung dose (e.g., FPD<3μm in **Table I** or $TLD_{in\ vitro}$ in **Table III**), formulation A-4.5 delivered less FP to the lung. The MMAD estimates in **Table I** are likely to suggest to an aerosol scientist that FP DPI formulations B-3.8 and C-3.7 might show a similar regional deposition pattern. In contrast, the larger MMAD of formulation A-4.5 might indicate a somewhat more central deposition. We thus achieved, at least in part, the goal to provide FP DPI formulations that might be suitable for probing whether PK is sensitive to differences in regional deposition.

Overall, the FP DPI formulations were stable at room temperature during the PK study period (from 12 to 20 months after storage at ambient conditions: 25°C, 60% RH; **Table II**) with only slight changes in the FPD during early storage (from 0 to 3 months at ambient conditions: 25°C, 60% RH). Based on compendial NGI *in vitro* experiments, the FP DPI formulation A-4.5 had a smaller DD_{NGI} (**Tables I** and **II**) than the other two formulations.

When considering the total dose delivered to the lungs, parameters such as the FPD < 3 μm, FPD < 5 μm, and $TLD_{in\ vitro}$ were assessed using the compendial NGI and the realistic *in vitro* testing (**Tables I** and **III**). These parameters also differed between the FP DPI formulations indicating that the total lung dose may have differed between the formulations in the PK study. To account for these differences in total *in vitro* DD, dose normalization of the PK data analysis was necessary. When evaluating regional dose delivery within the lungs, results of cascade impactor studies might be worthwhile to be considered. The drug amount deposited on NGI stages 2 to 3 (cut-off values are 4.46 and 2.82 μm, respectively) was comparable between the formulations (**Fig. 1, Table I**). This may indicate that similar doses might have reached the central lung (although a fraction of stages 2–3 will be certainly deposited in the mouth and throat region). Thus, similar amounts of FP from the DPI formulations might be exposed to mucociliary clearance. In contrast, NGI stages 4 to 7 (cut-off values of stages 4, 5, 6, and 7 are 1.66, 0.94, 0.55, and 0.31 μm, respectively) showed considerably lower amounts of drug deposition for formulation A-4.5 than those for formulations B-3.8 and C-3.7. Differences in the MMADs are associated predominantly with this fraction of the generated aerosol.

The total *in vitro* lung dose ($TLD_{in\ vitro}$) was subsequently determined using the three realistic, anatomical MT models (16, 17, 33–35) and one inhalation profile. These experiments indicated that $TLD_{in\ vitro}$ for a specific FP DPI formulation, but also the TLD ratios between two formulations, differed across the three MT models (**Table III**). Given the anatomical differences incorporated into each MT model, one might argue that differences between MT models likely also exist across human volunteers. Thus, one might discuss that a range of MT models might better capture "reality" for BE purposes. Based on these considerations, the *a priori* data analysis plan specified averaging the $TLD_{in\ vitro}$ (in μg) from the three MT models and using the resulting ratios for dose normalization of the PK study data. Considerable differences between the $TLD_{in\ vitro}$ estimates for different MT models introduced some uncertainty regarding the applied average normalization factors. Therefore, conclusions based on the dose-normalized BE results carry this uncertainty.

Such differences between MT models' performance were smaller in a study of budesonide DPIs (17), but our observations were similar to those reported for a suspension-based metered dose inhalers (36). Future *in vitro*/*in vivo* correlations are warranted to elucidate the differences in MT models' performance. At this time, considering the average of dose normalization factors obtained with the three MT models (**Table III**) for adjusting (i.e., dose normalizing) the PK parameters (C_{max}, AUC_{0-last} and AUC_{0-Inf}) seems a reasonable strategy to adjust for differences in the pulmonary deposited dose between the FP DPI formulations studied in this work.

For lipophilic drugs with low aqueous solubility such as FP, the fate in the lung (i.e., where drug lands at the site of action in the lung) and clinical efficacy are affected by its dissolution rate (22, 37). These differed across the FP DPI formulations studied in this work. As all three DPI formulations used FP (the API) from the same supplier, same batch, and same particle size distribution, different lactose fines caused the differences in MDT with formulation A-4.5 being the slowest (**Table I**). This suggested that lactose fines were responsible for a selective modulation of the API particle surface, presumably due to differences in the agglomerate microstructure. Thereby, lactose fines affected both pre-deposition and post-deposition events. This is important for interpretation of the C_{max} differences, since both slower dissolution and more central lung deposition may lead to lower C_{max}.

The design of the PK study allowed the assessment of both between-subject variability (BSV) and within-subject variability (WSV); the latter is not generally available from conventional published literature on PK BE studies. In this PK study, BSV was, on average, 33.5% for C_{max} and 24.1% for AUC_{0-Inf}. The WSV had generally small coefficients of variation (CV) of 28.7% for C_{max} and 14.6% for AUC_{0-Inf}.

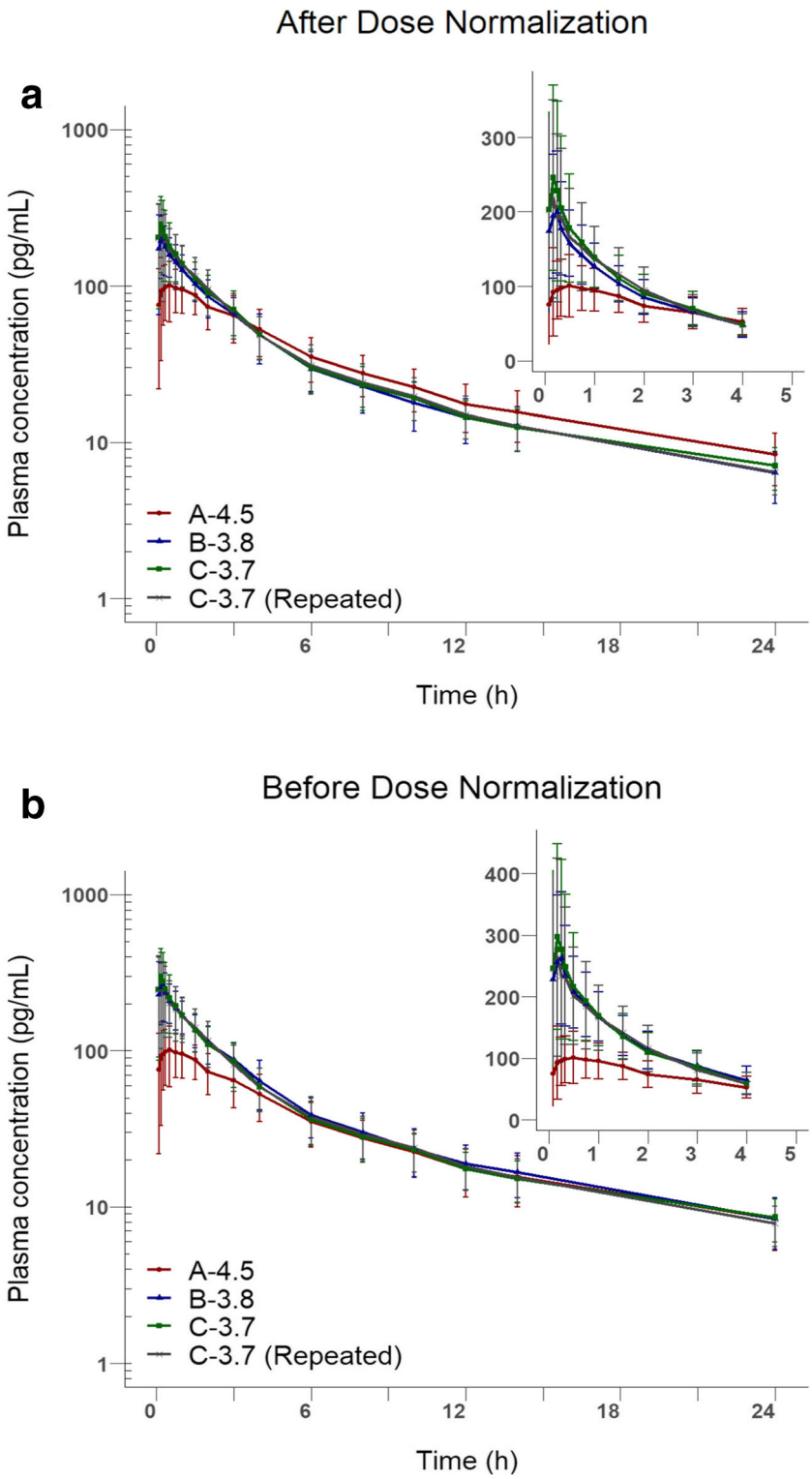

Figure 3. Plasma concentrations (mean ± standard deviation of FP DPI formulations A-4.5, B-3.8, and C-3.7 after (**a**) and before (**b**) dose normalization using $TLD_{in\ vitro}$. The insets show the first 4 h on linear scale

The intensive oral inhalation training of the healthy subjects by experienced, well-trained clinical staff team members; the strategy of at least two inhalations per capsule; and the ease of use of the DPI device likely contributed to these small variabilities. This yielded reproducible peak inspiratory flow rates across the 988 profiles (PIFR= 120 L/min, CV% 16.2%) collected during the conduct of PK study. The WSV estimates for AUC in this PK study were considerably smaller than few available WSV estimates for salbutamol (WSV: 32–52%) (38) or insulin (27%) (39). Knowledge of WSV under these

Table V. Non-compartmental PK Parameter Estimates for Fluticasone Propionate (FP) in Plasma

PK parameters	Unit	FP DPI formulations			
		A-4.5	B-3.8	C-3.7	C-3.7 (repeated)
Before dose normalization					
$t_{1/2}$	h	10.3 (5.74–17.6)	10.3 (6.88–13.4)	9.75 (6.33–15.6)	10.1 (6.74-19.9)
T_{max}	h	0.51 (0.18–1.60)	0.33 (0.17–1.10)	0.30 (0.17–1.08)	0.27 (0.17-1.10)
MRT	h	11.6 (6.46–18.1)	9.47 (7.07–13.7)	9.41 (6.23–13.7)	9.49 (6.28-16.5)
C_{max}	pg/mL	119 [100, 143]	286 [239, 342]*	275 [230, 329]*	308 [258, 368]*
$AUC_{0–last}$	pg.h/mL	658 [585, 740]	921 [819, 1036]*	868 [772, 977]*	907 [806, 1021]*
$AUC_{0–Inf}$	pg.h/mL	782 [696, 878]	1,040 [926, 1168]*	980 [873, 1101]*	1,035 [922, 1163]*
After dose normalization based on $TLD_{in\ vitro}$					
C_{max}	pg/mL	119 [100, 143]	217 [182, 260]*	227 [190, 271]*	254 [213, 304]*
$AUC_{0–last}$	pg.h/mL	658 [585, 740]	700 [622, 787]	716 [636, 805]	748 [665, 841]*
$AUC_{0–Inf}$	pg.h/mL	782 [696, 878]	790 [703, 888]	808 [719, 908]	853 [760, 959]

$t_{1/2}$ terminal half-life, T_{max} time to peak concentrations, *MRT* mean body residence time, C_{max} observed peak concentration in plasma, $AUC_{0–last}$ area under the plasma concentration time curve from time zero until the last observed plasma concentration, $AUC_{0–Inf}$ area under the plasma concentration time curve from time zero until time infinity. *Significantly different ($p<0.05$) from the estimate for FP DPI formulation A-4.5
Data represent median (min-max) or geometric mean [90% CI]

optimized conditions will be helpful for the design of future PK BE studies.

The FP DPI formulation A-4.5 had the smallest $TLD_{in\ vitro}$, slowest dissolution rate, and lowest C_{max} and $AUC_{0–Inf}$ (**Fig. 3, Table V**). In contrast, the more similar *in vitro* deposition attributes for the FP DPI formulations B-3.8 and C-3.7 resulted in comparable PK properties of these two formulations. The C_{max} occurred later for the FP DPI formulation A-4.5 supporting the notion of a longer MRT (**Table V**). This could have been caused by either a slower dissolution (due to potential differences in formulation microstructure, e.g., API-API vs. API-lactose agglomerates) or more central lung deposition of FP DPI formulation A-4.5. Given the same average terminal half-life for all formulations, the mean absorption time was likely longer for formulation A-4.5 compared to the other two formulations. Moreover, absorption of FP was found to be slower from the more central bronchiolar and bronchial airways in an animal model (10, 40). Without dose normalization, the present results support previous simulation work (9) in the context that a PK study should be able to detect differences in pulmonary available dose ($AUC_{0–Inf}$) and pulmonary residence time

Table VI. Bioequivalence Results Before and After Dose Normalization Using $TLD_{in\ vitro}$.

Before dose normalization	FP DPI formulations		Geometric mean ratio (test/reference)	
	Reference	Test	Point estimate	90% confidence interval
C_{max}	A-4.5	B-3.8	2.39	(2.09–2.74)[#]
	A-4.5	C-3.7	2.30	(2.01–2.64)[#]
	A-4.5	CR-3.7	2.58	(2.25–2.96)[#]
$AUC_{0–last}$	A-4.5	B-3.8	1.40	(1.31–1.50)[#]
	A-4.5	C-3.7	1.32	(1.23–1.41)[#]
	A-4.5	CR-3.7	1.38	(1.29–1.48)[#]
$AUC_{0–Inf}$	A-4.5	B-3.8	1.33	(1.24–1.43)[#]
	A-4.5	C-3.7	1.25	(1.17–1.35)[#]
	A-4.5	CR-3.7	1.32	(1.23–1.42)[#]
After dose normalization	**DPI formulations**		**Geometric mean ratio (test/reference)**	
	Reference	**Test**	**Point estimate**	**90% confidence interval**
C_{max}	A-4.5	B-3.8	1.82	(1.59–2.08)[#]
	A-4.5	C-3.7	1.90	(1.66–2.17)[#]
	A-4.5	CR-3.7	2.13	(1.86–2.44)[#]
$AUC_{0–last}$	A-4.5	B-3.8	1.06	(0.99–1.14)
	A-4.5	C-3.7	1.09	(1.02–1.16)
	A-4.5	CR-3.7	1.14	(1.06–1.22)
$AUC_{0–Inf}$	A-4.5	B-3.8	1.01	(0.94–1.08)
	A-4.5	C-3.7	1.03	(0.96–1.11)
	A-4.5	CR-3.7	1.09	(1.02–1.17)

[#] Not bioequivalent (90% confidence interval outside the 80.00 to 125.00% limits)

(C_{max}, T_{max}). These are two important factors relevant for the BE assessment of OIDPs.

As pre-specified in the SAP of the PK study, the PK data were normalized for differences in $TLD_{in\ vitro}$ to probe whether dose-normalized $AUC_{0–Inf}$ and C_{max} are sensitive to differences in the regional deposition. However, this was hampered by uncertainty regarding the DNF due to differences in $TLD_{in\ vitro}$ estimates from the three MT models (**Table III**). Previous simulation work (9, 41) and PK studies in asthmatic subjects (11) supported the hypothesis that more centrally deposited FP should result in a smaller $AUC_{0–Inf}$ since undissolved particles would be more efficiently removed through mucociliary clearance from the central portions of the lung. When using the DNF derived from $TLD_{in\ vitro}$ estimates (the $TLD_{in\ vitro}$ average of the three MT models was used, **Table III**), the FP DPI formulation A-4.5 still showed a trend towards an approximately 10% smaller $AUC_{0–Inf}$ compared to the other two formulations. However, these differences were not statistically significant, and formulation A-4.5 was found bioequivalent to formulations B-3.8 and C-3.7 for $AUC_{0–Inf}$ (**Table VI**). This might indicate that the difference in the MMAD was not sufficient and/or that the dose adjustment method (average of the three anatomical MT models) was not fully accurate.

We further hypothesized that differences in the regional lung deposition may be indicated by different dose-normalized C_{max} estimates, as a more central deposition would result in a slower absorption and lower C_{max}. The FP DPI formulation A-4.5 yielded substantially lower C_{max}, and this difference remained after dose normalization. We believe that these C_{max} differences were caused by a slower dissolution rate of formulation A-4.5 (**Table I**) due to potential differences in the formulation microstructure of agglomerated particles and its effects on dissolution relevant to API surface area. However, the impact of a slower dissolution rate for the FP DPI formulation A-4.5 was found to be too small to adequately explain the observed differences in dose-normalized C_{max} (42). Future physiologically based pharmacokinetic (PBPK) and population PK (popPK) modeling analyses are warranted to further investigate these factors. However, even without such advanced modeling analyses, some useful conclusions can be drawn.

The MDT of FP DPI formulation A-4.5 was 1.3 fold longer than that of formulation C-3.7, the formulation dissolving the fastest. Considering a direct relationship between MDT and mean absorption time (MAT) for slowly dissolving inhaled corticosteroids (22), one could ask how much higher the C_{max} would be if formulation A-4.5 would be absorbed with the absorption/dissolution rate of formulation C-3.7. We assumed that dissolution was the rate-limiting step for pulmonary absorption. We then considered the differences in MDT between FP DPI formulations A-4.5 and C-3.7 (**Table I**; MDT-USP: 23.4/17.8 = 1.3; MDT-Transwell: 12.2 h/8.5 h = 1.4) or the different kd estimates obtained from the USP paddle apparatus (0.076 h^{-1}/0.049 h^{-1} = 1.55). The two-compartment PK simulations module for FP (see "MATERIALS AND METHODS") was used to predict what C_{max} could be expected for FP DPI formulation A-4.5 if dissolution would occur at the rate as that observed for formulation C-3.7. In this simulation, C_{max} was predicted to increase only by 19 to 34%. This suggested that the much more pronounced C_{max} differences after dose normalization (1.9 or 1.8 fold larger estimate for formulations B-3.8 and C-3.7 compared to that of A-4.5) might be related to differences in regional lung deposition. This would be in agreement with our hypothesis that less drug was delivered by formulation A-4.5 to the more permeable peripheral parts of the lung (43). Future detailed analyses leveraging PBPK and popPK modeling are warranted to further underpin this hypothesis.

CONCLUSION

In this work, supported by *in vitro* experiments that characterized the $TLD_{in\ vitro}$ and dissolution rate of three FP DPI formulations, non-compartmental analysis indicated that PK was able to identify differences in the (1) pulmonary deposited dose before dose normalization and (2) pulmonary residence time after dose normalization (C_{max}/DNF, T_{max}). The hypothesis that PK can identify differences in the regional lung deposition through comparison of AUC estimates was hampered by not fully achieving the intended FP DPI formulation properties (i.e., same lung dose and same dissolution rate but with distinct differences in MMAD). We further observed difficulties in determining reliable pulmonary deposited dose estimates through *in vitro* methods. Thus, the AUC-based evaluations are not definitive at this stage. The performed PK simulations might indicate that differences in exposure (i.e., $AUC_{0–Inf}$) adjusted C_{max} values might not be solely explained by the observed dissolution rate differences for the three FP DPI formulations evaluated in this work. However, a more detailed, future analysis of the data will need to be performed to further strengthen the hypothesis that C_{max} is sensitive to differences in regional pulmonary deposition. In summary, PK has the potential to provide supportive insights on pulmonary performance characteristics of OIDPs (i.e., available dose, residence time, and, with reasonable likelihood, also regional deposition). While these results support generic drug development and BE evaluation of OIDPs, further modeling analyses supporting this conclusion are warranted and will be presented in future communications.

FUNDING

Funding for this work was made possible, in part, by the US Food and Drug Administration through contracts HHSF223201110117A and HHSF223201610099C and grants 1U01FD004950 and 1U01FD005231.

Research reported in this publication was supported by the National Center for Advancing Translational Sciences of the National Institutes of Health under Award Number UL1TR001427.

DECLARATIONS

Disclaimer Views expressed in this article are from the authors and do not necessarily reflect the official policies of the Department of Health and Human Services, the National Institutes of Health, and the FDA, nor does any mention of trade names, commercial practices, or organization imply endorsement by the US Government.

REFERENCES

1. Draft guidance on Fluticasone Propionate; Salmeterol Xinofoate. U.S. Department of Health and Human Services, Food and Drug Administration, Center for Drug Evaluation and Research (CDER); 2013.
2. Draft guidance on formoterol fumarate; mometasone furoate. U.S. Department of Health and Human Services, Food and Drug Administration, Center for Drug Evaluation and Research (CDER); 2016.
3. Draft guidance on beclomethasone dipropionate; mometasone furoate. U.S. Department of Health and Human Services, Food and Drug Administration, Center for Drug Evaluation and Research (CDER); 2018.
4. Masoli M, Weatherall M, Holt S, Beasley R. Systematic review of the dose-response relation of inhaled fluticasone propionate. Arch Dis Child. 2004;89(10):902–7.
5. Barnes PJ, Pedersen S, Busse WW. Efficacy and safety of inhaled corticosteroids. New developments. Am J Respir Crit Care Med. 1998;157(3 Pt 2):S1–53.
6. Lee SL, Saluja B, Garcia-Arieta A, Santos GM, Li Y, Lu S, et al. Regulatory considerations for approval of generic inhalation drug products in the US, EU, Brazil, China, and India. AAPS J. 2015;17(5):1285–304.
7. FDA. FYs 2013-2017 Regulatory science report: locally-acting orally inhaled and nasal drug products. https://www.fda.gov/drugs/generic-drugs/fys-2013-2017-regulatory-science-report-locally-acting-orally-inhaled-and-nasal-drug-products. Accessed 9 Mar 2021.
8. Adams WP, Ahrens RC, Chen ML, Christopher D, Chowdhury BA, Conner DP, et al. Demonstrating bioequivalence of locally acting orally inhaled drug products (OIPs): workshop summary report. J Aerosol Med Pulm Drug Deliv. 2010;23(1):1–29.
9. Weber B, Hochhaus G. A systematic analysis of the sensitivity of plasma pharmacokinetics to detect differences in the pulmonary performance of inhaled fluticasone propionate products using a model-based simulation approach. AAPS J. 2015;17(4):999–1010.
10. Boger E, Ewing P, Eriksson UG, Fihn BM, Chappell M, Evans N, et al. A novel in vivo receptor occupancy methodology for the glucocorticoid receptor: toward an improved understanding of lung pharmacokinetic/pharmacodynamic relationships. J Pharmacol Exp Ther. 2015;353(2):279–87.
11. Harrison TW, Tattersfield AE. Plasma concentrations of fluticasone propionate and budesonide following inhalation from dry powder inhalers by healthy and asthmatic subjects. Thorax. 2003;58(3):258–60.
12. Olsson B, Bondesson E, Borgström L, Edsbäcker S, Eirefelt S, Ekelund K, et al. Pulmonary drug metabolism, clearance, and absorption. In: Hickey AJ, Smyth HDC, editors. Controlled Pulmonary Drug Delivery. New York: Springer; 2011. p. 21–50.
13. United States Pharmacopeial Convention. General chapter <905> Uniformity of Dosage Units. United States Pharmacopeia and national formulary (USP 41-NF36). Rockville: United States Pharmacopeial Convention; 2016.
14. United States Pharmacopeial Convention. General chapter <601> aerosols, nasal sprays, metered dose inhalers, and dry powder inhalers. United States Pharmacopeia and national formulary (USP 41-NF36). United States Pharmacopeial Convention: Rockville; 2016.
15. Costa P, Sousa Lobo JM. Modeling and comparison of dissolution profiles. Eur J Pharm Sci. 2001;13(2):123–33.
16. Wei X, Hindle M, Delvadia RR, Byron PR. In vitro tests for aerosol deposition. V: using realistic testing to estimate variations in aerosol properties at the trachea. J Aerosol Med Pulm Drug Deliv. 2017;30(5):339–48.
17. Wei X, Hindle M, Kaviratna A, Huynh BK, Delvadia RR, Sandell D, et al. In vitro tests for aerosol deposition. VI: realistic testing with different mouth-throat models and in vitro-in vivo correlations for a dry powder inhaler, metered dose inhaler, and soft mist inhaler. J Aerosol Med Pulm Drug Deliv. 2018;31:358–371.
18. Xi J, Longest PW. Transport and deposition of micro-aerosols in realistic and simplified models of the oral airway. Ann Biomed Eng. 2007;35(4):560–81.
19. Burnell PK, Asking L, Borgström L, Nichols SC, Olsson B, Prime D, et al. Studies of the human oropharyngeal airspaces using magnetic resonance imaging IV—the oropharyngeal retention effect for four inhalation delivery systems. J Aerosol Med. 2007;20(3):269–81.
20. Mitchell J, Mark C, Sizer Y, Russell T, Solomon D. Adapting the Abbreviated Impactor Measurement (AIM) concept to make appropriate inhaler aerosol measurements to compare with clinical data: a scoping study with the “Alberta” Idealized Throat (AIT) inlet. J Aerosol Med Pulmon Drug Deliv. 2012;25(4):188–97.
21. Delvadia RR, Wei X, Longest PW, Venitz J, Byron PR. In vitro tests for aerosol deposition. IV: simulating variations in human breath profiles for realistic DPI testing. J Aerosol Med Pulm Drug Deliv. 2016;29(2):196–206.
22. Rohrschneider M, Bhagwat S, Krampe R, Michler V, Breitkreutz J, Hochhaus G. Evaluation of the Transwell system for characterization of dissolution behavior of inhalation drugs: effects of membrane and surfactant. Mol Pharm. 2015;12(8):2618–24.
23. Bhagwat S, Schilling U, Chen MJ, Wei X, Delvadia R, Absar M, et al. Predicting pulmonary pharmacokinetics from in vitro properties of dry powder inhalers. Pharm Res. 2017;34(12):2541–56.
24. Bulitta JB, Holford NHG. An introductory guide to non-compartmental analysis. In D'Agostino RB, Sullivan L, Massaro J (ed), Wiley Encyclopedia of Clinical Trials. Hoboken: John Wiley & Sons, Inc; 2008. p 1–28. https://doi.org/10.1002/9780471462422.eoct340.
25. Krishnaswami S, Möllmann H, Derendorf H, Hochhaus G. A sensitive LC–MS/MS method for the quantification of fluticasone propionate in human plasma. J Pharm Biomed Anal. 2000;22(1):123–9.
26. Krishnaswami S, Hochhaus G, Derendorf H. An interactive algorithm for the assessment of cumulative cortisol suppression during inhaled corticosteroid therapy. AAPS PharmSci. 2000;2(3):E22.
27. Kinnunen H, Hebbink G, Peters H, Shur J, Price R. An investigation into the effect of fine lactose particles on the fluidization behaviour and aerosolization performance of carrier-based dry powder inhaler formulations. AAPS PharmSciTech. 2014;15(4):898–909.
28. Kinnunen H, Shur J, Hebbink G, Muresan AS, Price R. Investigations into the relationship between lactose fluidization properties, device resistance and dry powder inhaler performance. In Dalby, RN, Byron, PR, Peart, J, Suman, JD, Farr, SJ and Young, PM (ed), RDD Conference Paper; 2010. p 791–794.
29. Kinnunen H, Hebbink G, Peters H, Huck D, Makein L, Price R. Extrinsic lactose fines improve dry powder inhaler formulation performance of a cohesive batch of budesonide via agglomerate formation and consequential co-deposition. Int J Pharm. 2015;478(1):53–9.
30. Jones MD, Santo JG, Yakub B, Dennison M, Master H, Buckton G. The relationship between drug concentration, mixing time, blending order and ternary dry powder inhalation performance. Int J Pharm. 2010;391(1-2):137–47.
31. Grasmeijer F, Lexmond AJ, van den Noort M, Hagedoorn P, Hickey AJ, Frijlink HW, et al. New mechanisms to explain the effects of added lactose fines on the dispersion performance of adhesive mixtures for inhalation. PLoS One. 2014;9(1):e87825.
32. Peng T, Lin S, Niu B, Wang X, Huang Y, Zhang X, et al. Influence of physical properties of carrier on the performance of dry powder inhalers. Acta Pharm Sin B. 2016;6(4):308–18.
33. Delvadia R, Hindle M, Longest PW, Byron PR. In vitro tests for aerosol deposition II: IVIVCs for different dry powder inhalers in normal adults. J Aerosol Med Pulm Drug Deliv. 2013;26(3):138–44.
34. Olsson B, Borgstrom L, Lundback H, Svensson M. Validation of a general in vitro approach for prediction of total lung

deposition in healthy adults for pharmaceutical inhalation products. J Aerosol Med Pulm Drug Deliv. 2013;26(6):355–69.
35. Zhang Y, Gilbertson K, Finlay WH. In vivo-in vitro comparison of deposition in three mouth-throat models with Qvar and Turbuhaler inhalers. J Aerosol Med. 2007;20(3):227–35.
36. Kaviratna A, Tian G, Liu X, Delvadia R, Lee S, Guo C. Evaluation of bio-relevant mouth-throat models for characterization of metered dose inhalers. AAPS PharmSciTech. 2019;20(3):130.
37. Hochhaus G, Mollmann H, Derendorf H, Gonzalez-Rothi RJ. Pharmacokinetic/pharmacodynamic aspects of aerosol therapy using glucocorticoids as a model. J Clin Pharmacol. 1997;37(10):881–92.
38. Aswania O, Ritson S, Iqbal SM, Bhatt J, Rigby AS, Everard ML. Intra-subject variability in lung dose in healthy volunteers using five conventional portable inhalers. J Aerosol Med. 2004;17(3):231–8.
39. Kapitza C, Hompesch M, Scharling B, Heise T. Intrasubject variability of inhaled insulin in type 1 diabetes: a comparison with subcutaneous insulin. Diabetes Technol Ther. 2004;6(4):466–72.
40. Boger E, Evans N, Chappell M, Lundqvist A, Ewing P, Wigenborg A, et al. Systems pharmacology approach for prediction of pulmonary and systemic pharmacokinetics and receptor occupancy of inhaled drugs. CPT Pharmacometrics Syst Pharmacol. 2016;5(4):201–10.
41. Weber B, Hochhaus G. A pharmacokinetic simulation tool for inhaled corticosteroids. AAPS J. 2013;15(1):159–71.
42. Hochhaus G. Using PBPK to link systemic PK to local delivery in the lung. American Society of Clinical Pharmacology and Therapeutics Annual Meeting. Washington: D.C; 2019.
43. Labiris NR, Dolovich MB. Pulmonary drug delivery. Part I: physiological factors affecting therapeutic effectiveness of aerosolized medications. Br J Clin Pharmacol. 2003;56(6):588–99.